

# Principles of networked weather radar operation at attenuating frequencies

V. Chandrasekar<sup>1</sup>, S. Lim<sup>1</sup>, N. Bharadwaj<sup>1</sup>, W. Li<sup>1</sup>, D. McLaughlin<sup>2</sup>, V. N. Bringi<sup>1</sup>, and E. Gorgucci<sup>3</sup>

<sup>1</sup>Colorado State University, Fort Collins CO, 80523, USA

<sup>2</sup>University of Massachusetts, Amherst, MA, USA

<sup>3</sup>National Research Council of Italy, Rome, Italy

## 1 Introduction

Conventional meteorological radars provide coverage for long ranges (often hundreds of kilometers) and support weather surveillance and hydrological monitoring applications by using high power transmitters and mechanically scanned antennas. These systems operate at wavelengths in 5–10 cm range in order to minimize attenuation due to precipitation, and this necessitates the use of physically large antennas to achieve good resolution at distant ranges. Research radars with observations at short ranges have demonstrated great potential for “targeted applications” such as tornado detection and flash flood monitoring. Therefore it would be desirable to develop radar systems for targeted applications.

The usefulness of radar to a specific application is heavily dependent on the accuracy and resolution of coverage. A fundamental physical limit imposed by transmission from single radar is the problem of changing resolution as a function of range. In addition the lowest coverage altitude gets higher with range due to earth curvature. As an alternate solution, a networked radar environment concept has been proposed (Chandrasekar and Jayasumana, 2001; McLaughlin, 2001). The basic principle of the networked radar environment is to be able to provide good coverage, in terms of accuracy and resolution to a large area through a network of radars. In order to be able to provide “economically feasible” solution to this approach, meteorological radar operation must change from the “preferred” S band operation to higher frequencies (just as space borne weather radar systems). However there are new sets of problems at higher frequencies, the major one being the impact of attenuation due to precipitation. In addition the requirement for combining observation from multiple radars also provides additional sets of challenges.

The U.S National Science Foundation recently established an Engineering Research Center titled the Center for Collaborative Adaptive Sensing of the Atmosphere (CASA),

formed by a consortium of four universities namely (listed alphabetically), Colorado State university, University of Massachusetts (lead University), University of Oklahoma, and University of Puerto Rico and partnership with industry and government labs to create the underlying science and engineering basis for new paradigm of networked radars applied to hazardous localized weather detection, tracking, and predicting.

This paper describes the governing physical principles for operating a networked radar system at attenuating frequencies. Models of backscatter and forward scatter of precipitation volumes are studied to enable retrievals of intrinsic reflectivity and velocity. High-resolution observations from the CSU-CHILL radar are used to evaluate the impact of space/time variation of precipitation in a networked radar environment. Preliminary results of the analysis conducted at X band frequencies are presented.

## 2 Attenuation statistics for radar design at X-Band

Attenuation due to precipitation is perhaps one of the most important factors to be dealt with while developing radars at high frequencies such as X-band. X-band radars suffer electromagnetic wave attenuation due to rain. For X-band radar design it is important to characterize the possible attenuation for a given maximum range of operation. The only way to collect such data is from dual frequency radar system with matched beams, one at non-attenuating frequency and the other at attenuating frequency. This paper presents an indirect approach to build such statistics. Chandrasekar et al. (2002) discuss simultaneous observations of rain by dual polarization radars at S- and X-band. Chandrasekar et al. (1990) showed that specific attenuation ( $k_h^X$ ) at X-band can be predicted from specific differential phase ( $K_{dp}^S$ ) at S band. The relations between  $K_{dp}^S$  and  $k_h^X$  can be written:

$$k_h^X(r) \cong a_h K_{dp}^S \quad (1)$$

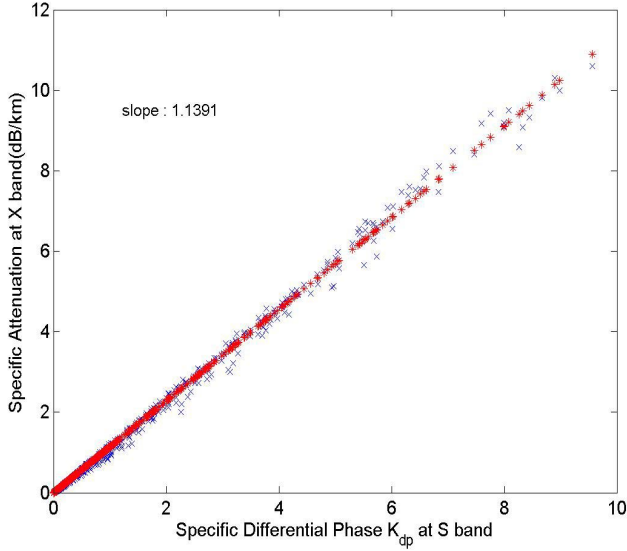


**Fig. 1.** Relationship between specific attenuation at X band and specific differential phase at S band for widely varying DSD.

where  $k_h^X$  is specific attenuation at X-band in horizontal polarization and  $K_{dp}^S$  is specific differential phase at S-band ( $\phi_{dp}$ ).

Figure 1 shows a scatter plot of  $k_h^X$  versus  $K_{dp}^S$  for widely varying raindrop size distribution. Based on the result shown in Fig.1, the cumulative attenuation at X-band  $A_h^X$  can be related to the differential propagation phase at S band as

$$A^X = 2 \int_0^R k_h^X(r) dr \approx 2 \int_0^R a K_{dp}^S(r) dr = a \Phi_{dp}^S \quad (2)$$

Two months of data collected by the CSU-CHILL radar (S-band) during the STEPS campaign (Severe Thunderstorm Electrification and Precipitation Study; conducted along the Colorado/Kansas border, May 26 ~Jul 19, 2000) collected by CSU-CHILL radar (S-band) were used in the estimation of the attenuation at X-band. For a given range, the cumulative density function of attenuation was calculated to compute the attenuation exceedance curves. Figure 2 shows the two-way attenuation statistics for the geographical region under study. Such statistics are useful in developing attenuation margin for X-band frequency. It can be seen that if the radar range is 30 km, 10% of precipitation cells will cause the attenuation beyond 19 dB.

### 3 Ground clutter

Radars designed for targeted applications at short ranges mitigate the earth curvature problem and provide finer resolution with smaller antennas compared to their S-band counterparts. Figure 3 (adopted from NRC 1995) shows the typical “lack of” low altitude coverage at far ranges. However radar observations at short ranges are contaminated by ground clutter. Ground clutter at close range could come from side lobes of the antenna or main lobe, depending on the radar altitude

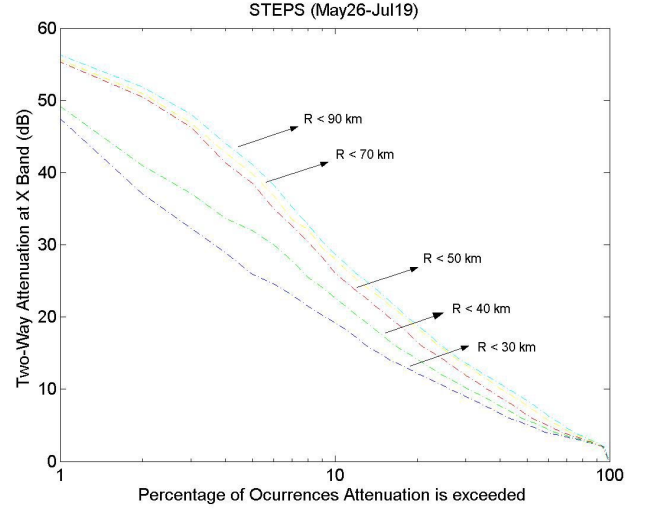


**Fig. 2.** Attenuation margin at X band frequency. Curves are obtained using data collected from various radar ranges, i.e. 30 km to 90 km. Attenuation statistics computed from differential phase observed by CSU-CHILL radar.

or the phenomena being observed. Specifically designing radars for short-range operation needs extensive emphasis for clutter mitigation. At close ranges the equivalent radar reflectivity due to clutter can easily be in the 40 to 60 dBZ range, whereas the phenomena being observed such as light rain or tornado may have echoes in the range of 20 to 40 dBZ. Therefore extreme care is needed for clutter mitigation.

### 4 Range-velocity ambiguity

Doppler weather radars transmitting pulses with uniform pulse repetition frequency (PRF) have a fundamental limitation on maximum unambiguous range ( $r_{max}$ ) and maximum unambiguous velocity ( $v_{max}$ ) given by

$$r_{max} v_{max} = \frac{c\lambda}{8}. \quad (3)$$

In Eq. (3)  $\lambda$  is radar wavelength and  $c$  is the velocity of light. Moving to higher frequencies such as X-band brings down the  $r_{max} v_{max}$  by a factor three compared to S-band. For example if  $r_{max}$  is kept at 150 km with a 1 millisecond pulse repetition time, the  $v_{max}$  at X-band drops to  $\pm 7.5$  m/s. There is always a trade off between  $r_{max}$  and  $v_{max}$  (Range-velocity ambiguity). Precipitation echoes can be distributed over a large area and the dynamic range of the radar reflectivity can be as high as 65 dB resulting in range overlay. Velocity measurements can span  $\pm 100$  m/s in severe storms resulting in velocity folding. Figure 4 shows the range-velocity limitation of an X-band radar compared to S-band radar.

X-band radars have a low unambiguous velocity due to their short wavelength, and increasing the PRF to mitigate this problem will result in multiple trip overlays as storms can extend over a large distance. It can be observed that

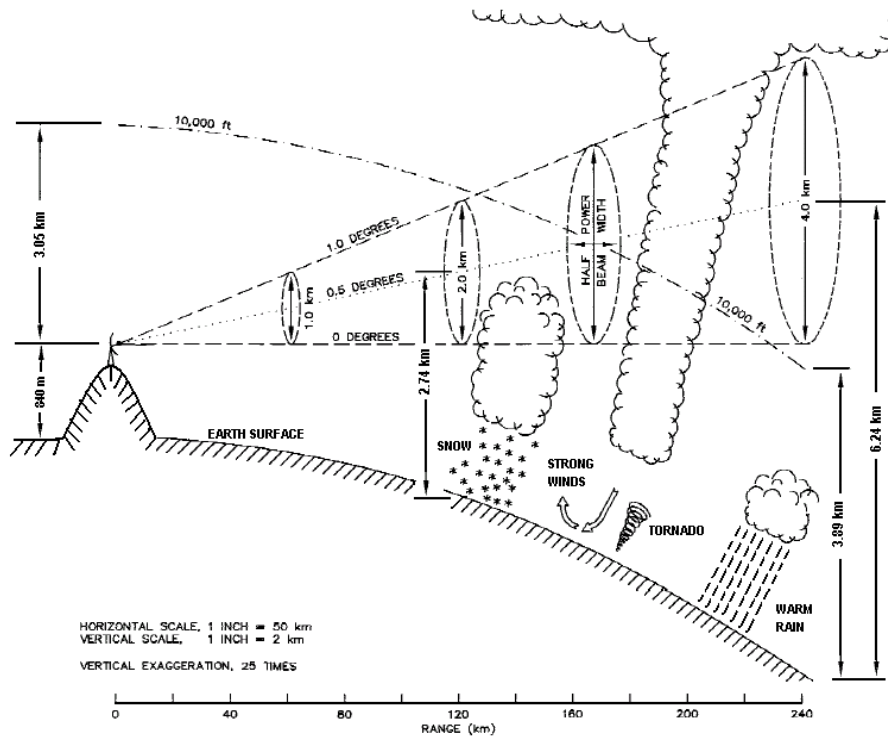


Fig. 3. The typical “lack of” low altitude coverage at far ranges (adopted from NRC 1995).

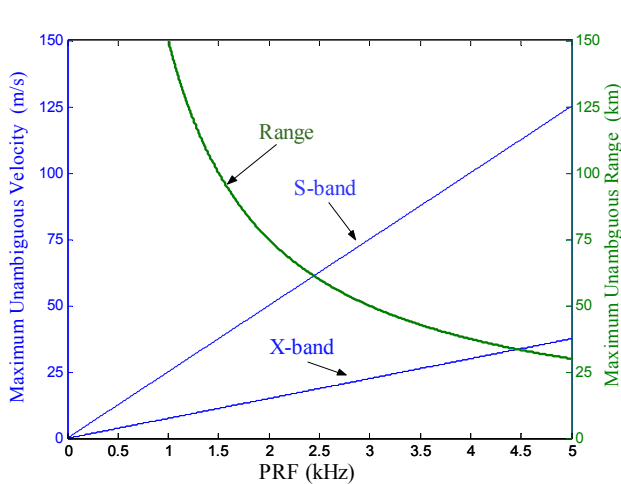


Fig. 4. Comparisons of range-velocity limitations for S-band and X-band radars.

range-velocity ambiguity is much more severe for X-band radars compared to the conventional S band.

Several range-velocity ambiguity mitigation schemes have been proposed. Staggered pulsing can be used to increase the unambiguous velocity whereas phase coding of the transmitted pulse can be used to mitigate range overlay (Zrnic and Mahapatra, 1985). Implementing these techniques for good performance at X-band is challenging and several solutions are being evaluated (Bharadwaj et al., 2004). All the above methods have been tested with S-band and C-band radars. Application to X-band is being evaluated.

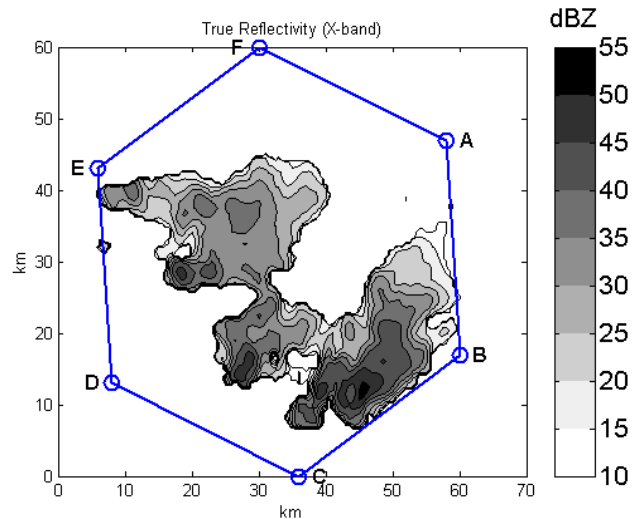
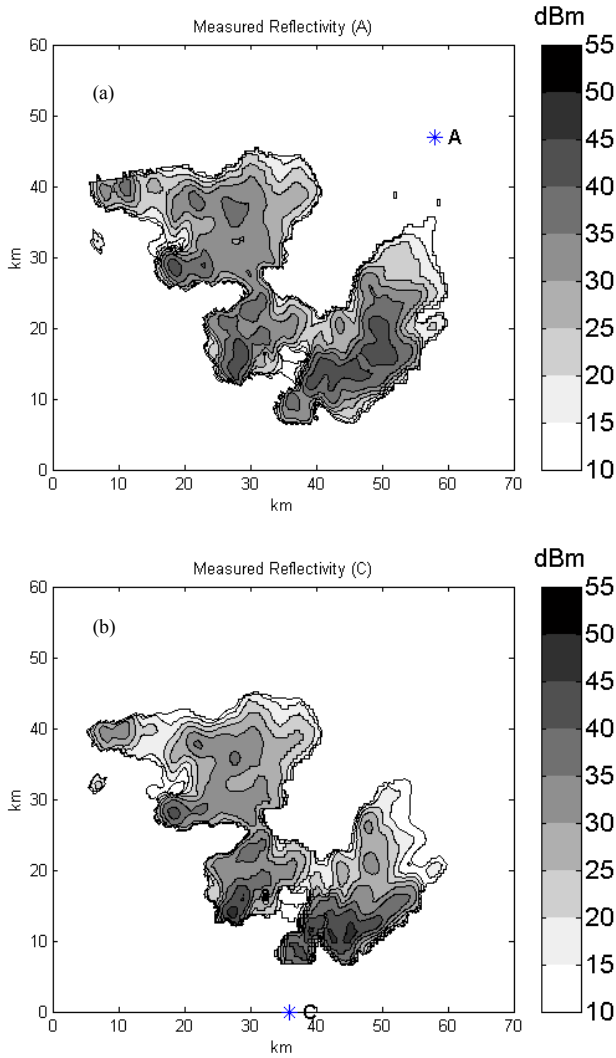


Fig. 5. Concept of networked radar environment.

### 5 Networked radar environment

Figure 5 shows the intrinsic reflectivity at X-band that was simulated from S-band observations. Figure 5 also shows a network of six radars A, B, C, D, E and F observing the same storm cell. Using a fairly accurate methodology to simulate X-band observations (Chandrasekar et al., 2004), Figs. 6a and b show the observations of the same storm by X-band radars located at A and C. The observed reflectivity by radars A and C is different than the intrinsic reflectivity shown in Fig. 5 because of path attenuation, which is dependent on the



**Fig. 6.** Measured reflectivity by radar A (a) and C (b).

location of the radar, storm and the rain path. The intrinsic radar reflectivity can be retrieved from these observations using a variety of methods and two which are discussed in the following section.

### 5.1 Attenuation correction using dual-polarization radar measurements

Differential phase measurements have been shown to be very useful for correcting the measured reflectivity for precipitation induced attenuation. This section describes two attenuation correction methodologies with specific emphasis on X-band. Simple differential phase based algorithm (DP) as well as the range-profiling algorithm based on differential phase constraints (DPC) were compared. Both of the algorithms for attenuation correction work fairly well (Bringi et al., 1990; Testud et al., 2000). Attenuation correction is required for any applications of radar data, such as feature detection algorithms, or rainfall estimation. Attenuation correction using reflectivity measurements alone, done iteratively from ranges

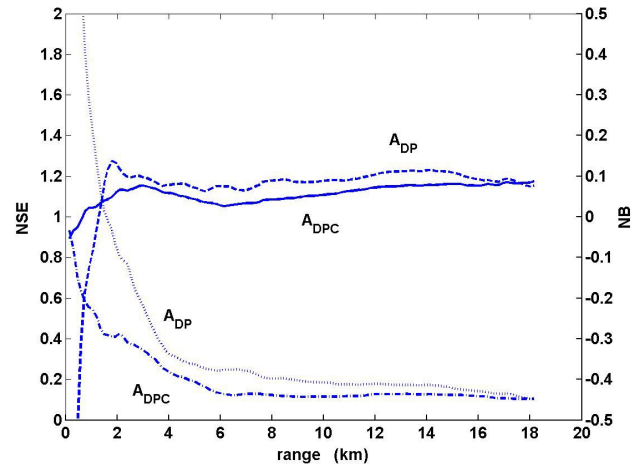


**Fig. 7.** Normalized Standard Error (left axis) and Normalized Bias (right axis) of cumulative attenuation, relative to X-band profiles based on S-band observations, as a function of range. The estimation of attenuation has been obtained using DPC and DP algorithms in presence of measurement errors.

close to the radars, were very unstable. Coherent polarization diversity radars brought significant advancements for attenuation correction in rain through the use of differential propagation phase. This ability has accelerated the consideration of X-band radars for rainfall monitoring.

The differential phase attenuation correction procedure (DP) is fairly simple to implement. The DPC method is not as simple, nevertheless easy to implement in modern processors. Regarding the correction of cumulative attenuation, both algorithms provide similar performance, with the differential phase constraint technique performing slightly better. Extensive study on these algorithms has been performed, and only summary of the results are provided for brevity. Both algorithms could keep the corrected reflectivity within  $\pm 1$  dB for 85% of the time, for the intense rain cells studied (Chandrasekar et al., 2004). In absence of measurement errors DP algorithm can provide much better estimates of the specific attenuation estimates compared to DPC method. However, practical issues associated with slope estimation reduce the resolution of the specific attenuation estimates, and suppress peaks. Figure 7 shows the normalized standard error (NSE) and bias of cumulative attenuation estimates for an 18 km rain path over intense precipitation. The NSE is defined as standard deviation normalized with respect to the mean. At short ranges the “absolute attenuation” is fairly small and the NSE is high due to that. For intense rain paths less than 10 km 95 % of the attenuation, corrected reflectivity stayed within  $\pm 1$  dB of the intrinsic value, demonstrating the ability of the differential phase based attenuation correction as well as DPC correction.

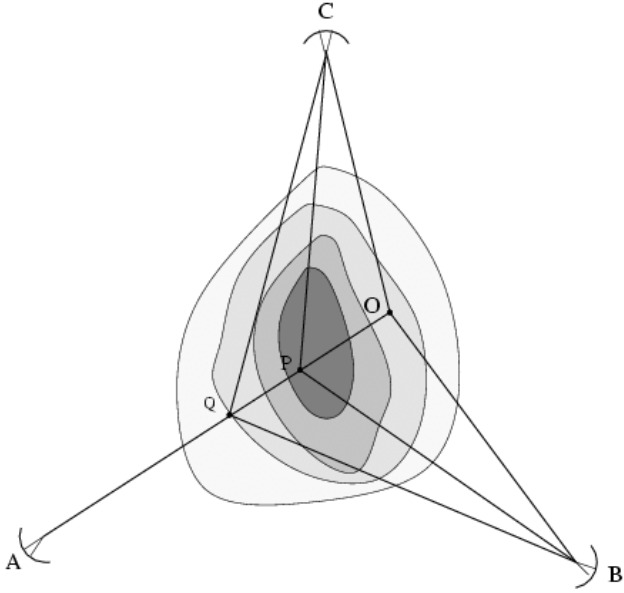


**Fig. 8.** Schematic showing the conceptual arrangement for reflectivity retrieval with networked radars.

## 5.2 Reflectivity retrieval in the networked radar environment

An alternate approach for to attenuation correction can directly use the networked radar approach. The specific attenuation distribution can be obtained from the integral equation for reflectivity, in a manner similar to that used with a differential phase constraint. The set of governing integral equations describing the backscatter and propagation properties of a common resolution volume are solved simultaneously with constraints on observed total path attenuation.

A three-radar network system is used for illustration as shown in Fig. 8. The retrieved reflectivity ( $Z_c(r)$ ) can be expressed in terms of the measured reflectivity ( $Z_m(r)$ ) and specific attenuation ( $k_h$ ) at range  $r$  as

$$Z_c(r) = Z_m(r) + 2 \int_{r_0}^r k_h(s) ds \quad (4)$$

If we know the intrinsic reflectivity ( $Z_e(r_m)$ ) at range  $r_m$ , the specific attenuation along the path can be described as

$$\Delta Z(r_m) = Z_e(r_m) - Z_m(r_m); \quad (5)$$

$$k_h(r) = \frac{[Z_m(r)]^b (10^{0.1b\Delta Z(r_m)} - 1)}{I(r_0; r_m) + (10^{0.1b\Delta Z(r_m)} - 1)I(r; r_m)}; \quad (6)$$

$$I(r_0; r_m) = 0.46b \int_{r_0}^{r_m} [Z_m(s)]^b ds \quad (7)$$

where  $\Delta Z(r_m)$  is the difference between intrinsic reflectivity and attenuated reflectivity, namely two-way cumulative attenuation, and parameter  $b$  corresponds to  $k - Z$  relation. A

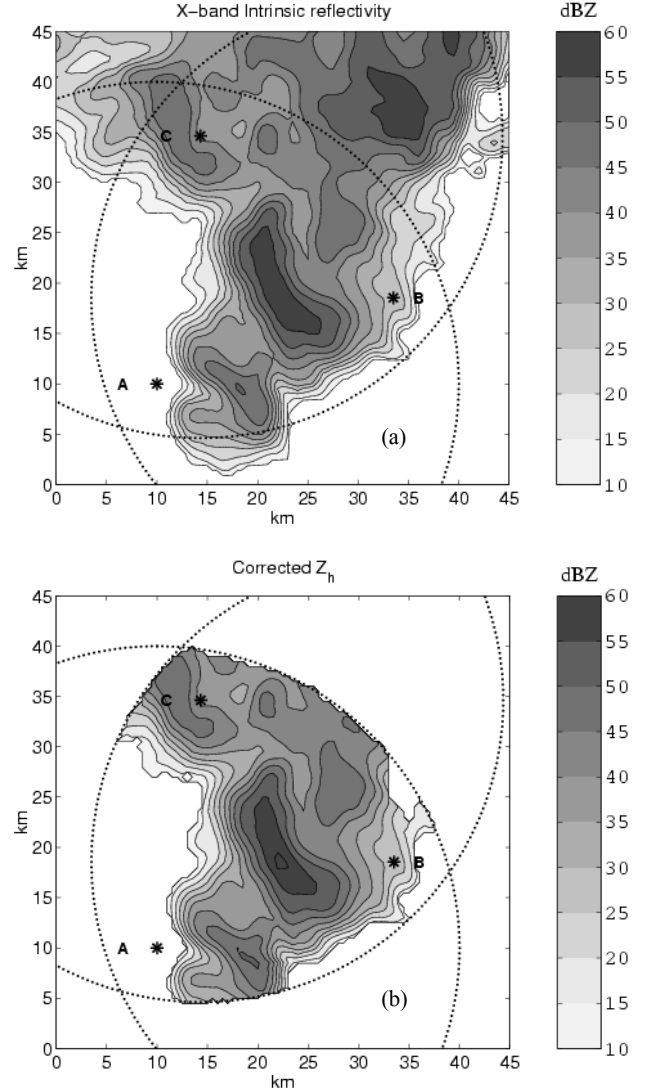


**Fig. 9.** (a) Intrinsic reflectivity and (b) retrieved reflectivity.

networked based solution is developed to solve for the intrinsic reflectivity and attenuation (Lim et al., 2004).

The optimum retrieved reflectivity at point  $O$  in Fig. 8 can be obtained by networked radar approach. Figure 9 shows the intrinsic reflectivity and retrieved reflectivity for common region by each radar, where as Fig. 10 shows the scatter plot of intrinsic reflectivity versus retrieved reflectivity. The standard deviation of the difference between intrinsic reflectivity and retrieved reflectivity is 0.62 dBZ, showing good performance.

## 6 Conclusions

Center for Collaborative Adaptive Sensing of the Atmosphere (CASA) is a consortium of universities, industry and government labs, established recently to develop the paradigm of networked radar environment, operating collaboratively adapting to the needs of the end users, as well as the

prevailing environment. The preliminary results shown here demonstrate that a distributed network approach, operating collaboratively adapting to the prevailing characteristics of precipitation can provide reasonable solutions to challenging problems such as retrieval of intrinsic reflectivity. Similar solutions are being pursued to resolve other challenges such as multi-dimensional Doppler retrieval and clutter mitigation, in order to enable operations at higher frequencies. Several generations of test beds will be developed with the initial one being a network of X-band radars with mechanically scanned antennas and the subsequent ones will include advances such as electronic scanning.

*Acknowledgement.* This research was supported by the National Science Foundation, Engineering Research Center Program (ERC-0313747). The authors acknowledge, the stimulating discussions with the large number of participants in CASA.

## References

- Bharadwaj, N., Chandrasekar, V., and Hubbert, J. C.: Staggered hybrid pulsing for polarimetric weather radars at X-band, Proceedings of IGARSS04, 2004.
- Bringi, V. N., Chandrasekar, V., Balakrishnan, N., and Zrnic, D. S.: An examination of propagation effects in rainfall on radar measurements at microwave frequencies, *J. Atmos. Oceanic Technol.*, 7, 829–840, 1990.
- Chandrasekar, V., Bringi, V. N., Balakrishnan, N., and Zrnic, D. S.: Error Structure of Multiparameter Radar and Surface Measurements of Rainfall, Part III: Specific Differential Phase, *J. Atmos. Oceanic Technol.*, 7, 621–629, 1990.
- Chandrasekar, V. and Jayasumana, A. P.: Radar Design and Management in a Networked Environment, Proceedings, ITCOMM, Denver CO, 142–147, 2001.
- Chandrasekar, V., Gorgucci, E., and Baldini, L.: Evaluation of polarimetric radar rainfall algorithms at X-band., ERAD02, 277–281, 2002.
- Chandrasekar, V., Gorgucci, E., Lim, S., and Baldini, L.: Simulation of X-Band Radar Observation of Precipitation from S-Band Measurements, Proceedings of IGARSS04, 2004.
- Lim, S., Chandrasekar, V., and McLaughlin, D.: Retrieval of reflectivity in a networked radar environment, Proceedings of IGARSS04, 2004.
- McLaughlin, D.: Presentation to “Weather Radar Technology Beyond Nexrad”, National Research Council, National Academy Press, Washington, D.C., 2001.
- NRC: Assessment of NEXRAD Coverage and Associated Weather Services, Washington, D.C., National Academy Press, 1995.
- Testud, J., Bouar, E. L., Obligis, E., and Ali-Mehenni, M.: The rain profiling algorithm applied to polarimetric weather radar, *J. Atmos. Oceanic Technol.*, 17, 322–356, 2000.
- Zrnic, D. S. and Mahapatra, P. R.: Two methods of ambiguity resolution in pulsed Doppler weather radars, *IEEE Trans. Aerospace and Electronic Systems.*, AES-21, 470–483, 1985.